Future Carbon Future

Full-composition jet fuel from CO_2 hydrogenation: interfacial reaction network engineering delivering on the e-SAF promise

Chenxi Zhang[1,2] and Fei Wei[1,2] ✉

[1] Beijing Key Laboratory of Green Chemical Reaction Engineering and Technology, Department of Chemical Engineering, Tsinghua University, Beijing, 100084, China
[2] Ordos Laboratory, Ordos 017010, China

Carbon Future 2026, 3, 9200088 https://doi.org/10.26599/CF.2026.9200088

Received: September 22, 2026; Accepted: September 23, 2026

✉ Corresponding author. Email: wf-dce@mail.tsinghua.edu.cn; ORCID: 0000-0002-1422-9784

Abstract

Aviation needs a fuel it cannot yet produce at scale, and direct CO_2 hydrogenation offers one of the shortest conditional routes to full-composition, drop-in electro-sustainable aviation fuel (e-SAF). The central constraint is no longer merely the Brønsted–Evans–Polanyi trade-off at an isolated site, but the architecture of a reaction network in which CO_2 activation, C–C coupling, aromatic formation, hydrogenation, and heat removal must cooperate. Interfacial reaction network engineering (IRNE) turns this into a design rule: an oxide domain activates C–O bonds, a zeolite domain drives C–C coupling and aromatization, and the two are coupled via controlled interfacial transfer of short-lived intermediates under a weak chemical-potential driving force. Recent kiloton-scale validation—high CO_2 conversion, high C_{8+} selectivity, low methane, and thousand-hour operation without oxidative regeneration—shows the "impossible triangle" of activity, selectivity, and stability can be relaxed when catalyst nanostructure and fluidized-bed hydrodynamics are co-designed. The remaining question is boundary-dependent rather than conceptual: whether cheap renewable electricity, low-cost carbon, million-tonne modules, and on-spec upgrading converge fast enough to make full-composition CO_2 fuel competitive. We close by identifying the operando descriptors, scale-sensitive economics, and open engineering questions that must now be settled.

Keywords

CO_2 hydrogenation; sustainable aviation fuel; e-SAF; interfacial reaction network engineering; $ZnCrO_x$/H-ZSM-5; high-pressure fluidized bed; process intensification; life-cycle boundary

1. Introduction

Aviation contributes only ~2.5% of global CO_2 emissions, yet non-CO_2 radiative forcing multiplies its climate impact two- to four-fold. With the sector committed to net-zero by 2050, sustainable aviation fuel (SAF) is expected to deliver more than 60% of the required abatement.[1] Meanwhile, the economics of the feedstocks are shifting beneath the debate: the levelised cost of solar and wind power has fallen dramatically, and electrolytic hydrogen is now ~40% cheaper than in 2020, approaching the cost of natural-gas-derived hydrogen.[20,22] The implementation gap for green hydrogen remains real, but for high-resource regions the learning curves now cross the deployment threshold.[20] We argue that this inflection point rewrites what is possible for CO_2 utilisation. Full-composition jet fuel—paraffins, cycloalkanes and aromatics assembled in a single fraction—is the most consequential of these products, because it is the only form of SAF that drops into the existing fleet without penalty. Direct CO_2 hydrogenation is among the shortest chemical paths to it.

2. Diagnosing the structural ceiling

Today's three SAF families each hit a structural ceiling. Hydroprocessed esters and fatty acids (HEFA) are capped by lipid availability: China's annual waste-oil supply of roughly 10 Mt cannot yield more than ~4 Mt of SAF. Fischer–Tropsch synthesis is capped by statistics: the Anderson–Schulz–Flory (ASF) distribution confines carbon efficiency to the jet cut and leaves the product short of the aromatic function that legacy airframes require.[2,5] Methanol-to-jet (MTJ) routes are capped by thermodynamics and process count: multiple equilibrium-limited steps demand four to six reactors and erode efficiency at each one. Direct CO_2 hydrogenation would bypass all three ceilings, but it confronts an "impossible triangle": high activity demands strongly reducing surfaces that over-hydrogenate CO_2 to methane; high selectivity demands acidic zeolite

confinement that cannot, by itself, activate CO_2; and high stability demands suppression of the aromatic polycondensation that the desired intermediates thermodynamically favour.[2–4] The diagnosis is architectural: mutually incompatible functions are confined to a single catalytic zone.[5]

3. A paradigm shift: interfacial reaction network engineering

Interfacial reaction network engineering (IRNE) resolves the triangle by changing the design unit—from the active site to the reaction network.[6,7] We use IRNE not as a synonym for bifunctional catalysis, but as a system-level design rule that specifies how catalyst domains, reactor hydrodynamics and boundary conditions must be co-designed. The nano-bifunctional catalyst supplies the elementary units; IRNE defines the network constraints under which those units remain coupled. Rather than breaking the Brønsted–Evans–Polanyi relation, IRNE circumvents it: an oxide domain such as $ZnCrO_x$ activates C–O bonds and supplies oxygenated or hydrogenated C_1 intermediates, whereas a zeolite domain such as H-ZSM-5 conducts C–C coupling, aromatization and shape-selective egress.[8-11,15] The two domains are not merely placed in proximity; they are coupled through a controlled interfacial flux of short-lived intermediates, driven by a weak chemical-potential jump between domains. The operating principle is therefore matched driving force: too little interfacial transfer loses intermediates to desorption or over-oxidation, whereas too much destroys selectivity by methane formation, uncontrolled C–C coupling or aromatic polycondensation.

Three descriptors make the design logic explicit; we state them as heuristics that require operando spectroscopy and microkinetic calibration rather than as settled laws. First, the entropy–time wall: for formaldehyde, ketene and surface CH_x species, the entropy penalty associated with desorption and the short surface lifetimes inferred near 623 K imply transfer lengths of order $\ell \approx \sqrt{(D\tau)}$, where

D is the surface/interfacial diffusivity and τ is the intermediate lifetime. Under the stated assumptions, transfer must occur before gas-phase escape, making interfacial spillover a kinetic necessity rather than an optional enhancement. Second, cascade dilution: rapid removal of oxygenated and hydrocarbon-pool intermediates by the downstream domain can hold the autocatalytic hydrocarbon pool below its polymerization threshold, reducing coking relative to a pure zeolite environment. Third, bidirectional cycling: partial back-transfer of aromatics and hydrogen equivalents from the zeolite to the oxide may sustain interfacial self-cleaning and moderate over-hydrogenation. These descriptors define a Goldilocks region: sufficient intimacy for spillover and desorption pumping, but not the over-coupling that would erase the distinct chemical functions of the two domains. Spatially, this logic must be expressed across hierarchical length scales—active sites at ångström–nanometre scale, nanodomain interfaces at several-to-tens of nanometres, spray-dried microspheres at tens of micrometres, and the high-pressure fluidized bed at metre scale. The optimal domain separation is not a universal constant; it depends on τ, D, pore architecture, aromatic back-flux, collision intensity and the critical hydrodynamic pressure of the fluidized bed.

4. From concept to kiloton-scale validation

These principles have now survived contact with engineering reality, but the evidence must be reported with explicit boundaries. In the CO2AF™ kiloton-scale demonstration—a 2 m × 10 m high-pressure fluidized bed operating at 350 °C and 3.5 MPa—spray-dried 50–100 μm microspheres containing $ZnCrO_x$ nanodomains and H-ZSM-5 nanosheets were reported to deliver high CO_2 conversion, high C_{8+} selectivity and low methane formation, with the carbon balance closing to ~99% and a single continuous run exceeding 1,000 hours without oxidative

regeneration.[12–14] This stability is consistent with the multilevel engineering principles identified for high-pressure fluidized beds. Critical fluidization pressure scales inversely with the square of particle diameter, $p_c \propto 1/d_p^2$. Approaching this critical pressure, bubbles vanish and the solid phase homogenizes; however, both collision frequency and heat/mass transfer rates then collapse—a "transfer-rate trap". Particle image velocimetry, residence time distribution and Peclet-number measurements delineate three regimes as a function of p/p_c.[13] The present operation falls in the intermediate regime: low inter-particle collision frequency while retaining high heat and mass transfer, which suppresses separation of the $ZnCrO_x$ and H-ZSM-5 active domains. These values should be read together with the earlier hundred-tonne pilot and process literature: CO_2 conversion above ~65%, heavy-aromatic selectivity above ~85 wt%, CO_2 recycle above ~95% and continuous operation beyond 1,000 hours established feasibility; the kiloton demonstration updates the scale and product-cut definition, not the underlying mechanism.[13] The important point for this article is not any single percentage. It is that cascade dilution and bidirectional cycling can be made to operate in a reactor whose hydrodynamics avoid both low-collision stagnation and high-collision separation of $ZnCrO_x$ and H-ZSM-5.

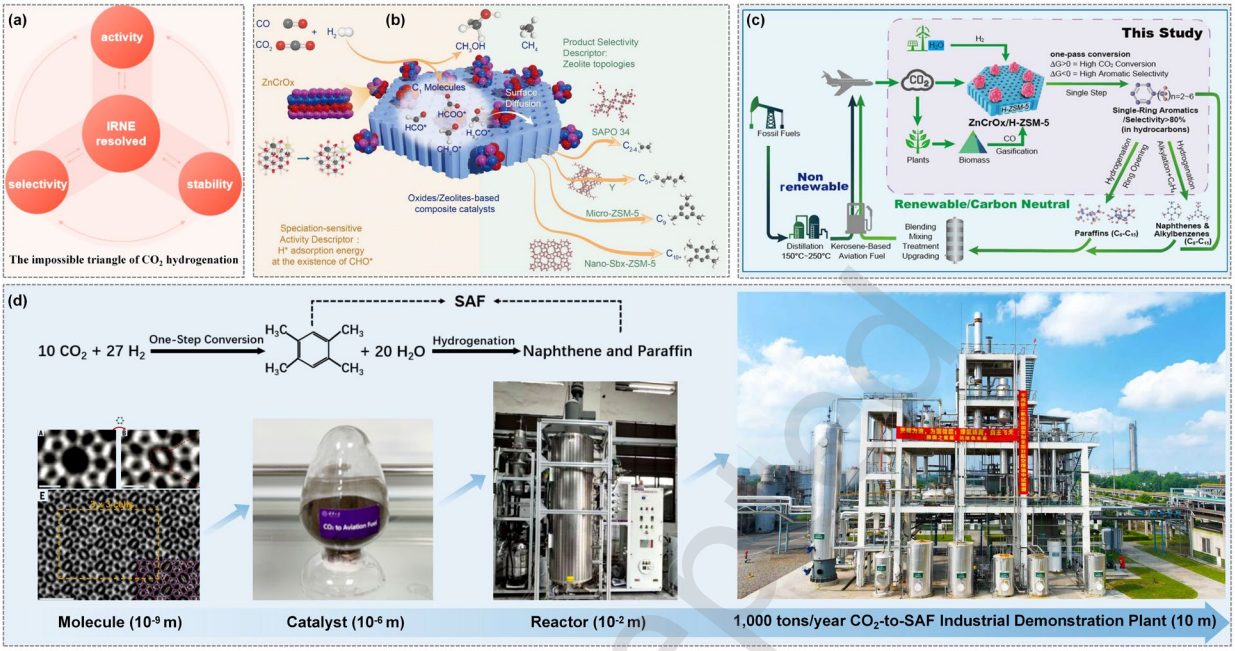

Fig. 1 | From the impossible triangle to a 1,000-tonne-per-year CO_2-to-SAF demonstration. (a) High activity, selectivity and stability resolved by IRNE. (b) $ZnCrO_x$ activates C–O bonds and H-ZSM-5 drives C–C coupling; controlled interfacial transfer channels intermediates to kerosene-fraction aromatics. (c) Renewable H_2 and captured CO_2 react in one step over $ZnCrO_x$/H-ZSM-5; hydrotreating upgrades the aromatic product to drop-in eSAF. (d) Scale-up from catalyst molecule (10^{-9} m) to demonstration plant.

5. The full-composition advantage under a unified boundary

The primary product is aromatic-rich—an asset only when the final fuel is defined on specification. Selective hydrogenation, ring-opening isomerisation and fractionation must convert it into a full-composition fuel (drop-in eSAF) that meets ASTM D7566 and Def Stan 91-091, carrying controlled aromatics for seal compatibility, a density near 790–810 kg m^{-3} and a freeze point below −50 °C. The hydrogen ledger is equally decisive. Because the pathway bypasses a separate reverse water-gas-shift reactor and because aromatic-ring products carry intrinsically lower H/C ratios, total hydrogen consumption can be reduced relative to CO_2-start FT-SPK and MTJ evaluated under the same CO_2 + H_2 boundary (Table 1). We are explicit about the scope: the advantage lies in carbon efficiency and process intensity, not thermodynamic transcendence; the well-to-wake

efficiency is earned through heat integration, scale and valorization of non-target cuts rather than assumed away.

Table 1 | Comparative metrics of e-SAF production routes from a CO_2 start under a unified CO_2 + H_2 boundary including CO_2 capture, synthesis, upgrading and delivery; syngas-based literature values corrected.

Metric (unified CO_2 + H_2 boundary)	**FT-SPK (CO_2 start)**	**MTJ (CO_2 start)**	**CO2AF™ (IRNE)**
Total H_2 consumption (Nm^3 t^{-1} fuel)	8000–9500	7500–8500	**5200–5300***
First-step H_2 (rWGS / CO_2→MeOH / direct)	+2240	+1800	**0 (bypasses rWGS)**
Carbon efficiency to C_{8}^{+} (%)	22–28	38–45	**72–75***
Well-to-wake energy efficiency (%)	32–38	40–48	**48–55***
Jet-fraction selectivity (%)	25–30	60–70	**90–93***
CH_4 selectivity (%)	8–15	3–5	**1.67–low***
Main reactors	4–5	5–6	**2**

**Boundary note. Values are conditional design targets rather than universal constants. Hydrogen consumption is reported as Nm^3 H_2 per tonne of final on-spec fuel and should be read with the same HHV/LHV basis, electrolyzer efficiency, compression duty, recycle configuration and upgrading yield across routes. "First-step H_2" denotes H_2 consumed before hydrocarbon synthesis, including reverse water-gas shift for syngas-based CO_2 routes or CO_2-to-methanol for MTJ-type routes; the IRNE/CO2AF route is credited with bypassing a separate rWGS reactor only when CO_2 activation and C–C coupling are integrated in one catalytic system. Carbon efficiency to C_{8}^{+} is defined on a converted-carbon basis unless otherwise stated; once-through values can be lower. Jet-fraction selectivity refers to the final on-spec C_8–C_{16} cut after hydrogenation, ring-opening/isomerization and fractionation, not merely primary heavy-aromatic selectivity. Well-to-wake efficiency assumes low-carbon renewable electricity and excludes policy credits; values are not directly comparable to life-cycle emissions unless electricity carbon intensity, CO_2 source and end-of-life treatment are specified. The central message is directional: CO2AF/IRNE improves carbon efficiency and process intensity by reducing methane, recycle demand and separate syngas-generation steps, but it does not transcend thermodynamics.*

6. China's window, and the decade ahead

The strategic prize is especially visible in China, where three assets converge: large volumes of capturable industrial CO_2, the world's most aggressive renewable-power and electrolyzer build-out, and a rapidly growing aviation market. With northwestern solar and wind power in the US$0.02–0.03 kWh^{-1} range, electrolyzers below roughly US$300 kW^{-1} and hydrogen potentially approaching ¥15 kg^{-1} by 2030 under continued learning, CO_2-derived full-composition fuel could enter a 0.8–1.2 US$ L^{-1} corridor earlier than in import-dependent markets. We stress that this is a conditional corridor, not an automatic outcome. It requires low-cost electricity, point-source CO_2 where available, modules at multi-hundred-kilotonne to million-tonne scale, carbon efficiency at or above ~70%, tight heat integration and on-spec upgrading. Under DAC-dominated, sub-10 kt

or weakly integrated boundaries, learning-curve analyses place e-SAF in a substantially higher cost range.[21–23] The policy implication is that blending mandates and carbon-market rules will open a supply gap that only feedstock-unconstrained routes can close, but they will not by themselves deliver parity; procurement, power-price contracts, CO_2 aggregation, standardization and scale-up must be coordinated.[16,17]

CO_2 governance in the coming decade should therefore be portfolio thinking. Catalytic hydrogenation is the highest-intensity option for full-composition fuel; biological or photobiological systems can complement it where land and water are genuinely available. Our photovoltaic-assisted desert-pond demonstration fixes CO_2 and produces lipid oil at promising areal rates, but the fixed carbon returns to the atmosphere on combustion: this is utilization, not storage, and algal lipids yield paraffinic, aromatics-free fuel that blends naturally with—not replaces—full-composition fuel.[18] Water, land and ecological impact, not photosynthetic imagination, are the binding constraints at scale.

Looking five to ten years ahead, we see three trajectories. First, CO2AF-type production should move from kiloton validation to multi-hundred-kilotonne and million-tonne modules in northwestern "golden-triangle" hubs that couple renewable power, point-source CO_2 and aviation demand, because scale-sensitive learning curves penalize small, distributed production of complex drop-in fuels. Second, life-cycle carbon intensity can approach zero and turn negative only when renewable electricity is genuinely additional, methane formation remains low, non-target cuts are valorized rather than burned, and durable carbon accounting is applied; credit prices above ~US$100 tCO_2^{-1} make the negative range plausible but not self-executing. Third, IRNE descriptors should migrate to other bifunctional catalytic systems, with AI-assisted catalyst and flowsheet

screening accelerating discovery but not substituting for operando evidence.[19] Five questions must stay on the community's agenda: quantitative operando calibration of the entropy–time, cascade-dilution and bidirectional-cycling descriptors; microsphere attrition, fines management and thousand-hour-plus stability in industrial high-pressure fluidized beds, including the transfer-rate trap near critical fluidization; first-principles microkinetic validation; dynamic integration with hydroprocessing under fluctuating renewable H_2 and CO_2 supply; and full life-cycle assessment including catalyst manufacture, solvent/sorbent replacement where relevant, and end-of-life.

Data availability

All data needed to evaluate the conclusions in the article are present in the article and/or the Supplementary Information. Demonstration values cited from project reports or accepted manuscripts are available from the corresponding author upon reasonable request.

Acknowledgements

We would like to thank the National Natural Science Foundation of China (22238004, 22278238), the Natural Science Foundation of Inner Mongolia Autonomous Region of China (2025JQ028), the Major Science and Technology Program of Inner Mongolia Autonomous Region (20212120326), "Elite Talents Revitalize Inner Mongolia" Initiative – Tier-1 Talent Team (2025TYL01), Ordos Science and Technology Breakthrough (JBGS2024003), Tsinghua University Initiative Scientific Research Program, Ordos-Tsinghua Strategic Cooperation Project on Technological Innovation and Ordos Laboratory (Ordoslab-kjzc-202501, Ordoslab-kjzc-202601) for their financial support.

Author contribution statement

Conceptualization: C. X. Zhang, F. Wei; methodology: C. X. Zhang, F. Wei; investigation: C. X. Zhang; validation: F. Wei; formal analysis: C. X. Zhang, F. Wei; writing—original draft: C. X. Zhang; writing—review and editing: C. X. Zhang, F. Wei; supervision: C. X. Zhang, F. Wei; funding acquisition: C. X. Zhang, F. Wei. All authors approved the final manuscript.

Competing interests

The authors have no competing interests to declare that are relevant to the content of this article.

References

[1] IATA. Net Zero by 2050: Sustainable Aviation Fuel. International Air Transport Association Roadmap, Montreal, 2021.

[2] Tian, G.. COx conversion to aromatics: a mini-review of nanoscale performance. *Nanoscale Horiz.* 2022.

[3] Li, Z.. Determination of Mn valence states in nanocatalysts during sustainable syngas conversion. *J. Am. Chem. Soc.* 2025, *147*, 32543–32559.

[4] Liao, D.. Toward an active site-performance relationship for oxide supported single and few atoms. *ACS Catal.* 2025, *15*, 8219–8229.

[5] Liang, B.. Thermodynamic insights into sustainable aviation fuel synthesis via CO/CO_2 hydrogenation. *Catalysts* 2023, *13*, 1396.

[6] Jiao, F.. Selective conversion of syngas to light olefins. *Science* 2016, *351*, 1065–1068.

[7] Cheng, K.. Direct and highly selective conversion of synthesis gas into lower olefins. *Angew. Chem. Int. Ed.* 2016, *55*, 4725–4728.

[8] Bligaard, T.. The Brønsted–Evans–Polanyi relation and the volcano curve in heterogeneous catalysis. *J. Catal.* 2004, *224*, 206–217.

[9] Arslan, M.. Highly selective conversion of CO_2 or CO into precursors for kerosene-based aviation fuel via an aldol-aromatic mechanism. *ACS Catal.* 2022, *12*, 2023–2033.

[10] Tian, G.. Accelerating syngas-to-aromatic conversion via spontaneously monodispersed Fe in $ZnCr_2O_4$ spinel. *Nat. Commun.* 2022, *13*, 5567.

[11] Tian, G.. Efficient syngas conversion via catalytic shunt. *Nat. Sustain.* 2025, *8*, 508–519.

[12] Wei, F.. Kiloton-scale CO_2 hydrogenation to sustainable aviation fuel via interfacial reaction network engineering. *Chin. J. Chem. Eng.* 2026, in press.

[13] Lu, F.. Road to carbon-neutral aviation: one-step conversion of CO_2 to sustainable aviation fuels. *Ind. Eng. Chem. Res.* 2025, *64*, 3118–3135.

[14] Lu, F.. High-pressure fluidization technology and applications. *Particuology* 2026, *117*, 104–121.

[15] Tian, G.. Upgrading CO_2 to sustainable aromatics via perovskite-mediated tandem catalysis. *Nat. Commun.* 2024, *15*, 3037.

[16] Tian, G.. Fueling the future: innovating the path to carbon-neutral skies with CO_2-to-aviation fuel. *Carbon Future* 2024, *1*, 9200010.

[17] European Commission. ReFuelEU Aviation—Regulation (EU) 2023/2405, 2023.

[18] CNPC. Microalgae biodiesel: an introduction (~170 t CO_2 ha^{-1} yr^{-1} fixation). China National Petroleum Corporation Popular Science, 24 May 2016 (in Chinese).

[19] Tian, G.. A dual-engine artificial intelligence framework accelerates sustainable aviation fuel component synthesis. *J. Am. Chem. Soc.* 2026, *148*, 9879–9891.

[20] Odenweller, A.. The green hydrogen ambition and implementation gap. *Nat. Energy* 2025, *10*, 110–123.

[21] Cheng, F.. Impacts of the Inflation Reduction Act on the economics of clean hydrogen and synthetic liquid fuels. *Environ. Sci. Technol.* 2023, *57*, 15336–15347.

[22] Dai, Y.. Use of learning curve to explore the competition between renewables and conventional fossil fuel power technologies in China. *Energy Strategy Rev.* 2024, *52*, 101352.

[23] Lackner, K. S.. Buying down the cost of direct air capture. *Ind. Eng. Chem. Res.* 2021, *60*, 8196–8208.